

Arsenic Removal from Groundwater Using Recycled Iron Nanoparticles: Development and Evaluation of a Low-Cost Filter for Rural Communities

Juan Simón Torres Espada^{1*} and Yrene Romina Lazcano Cruz¹

Summary

The presence of geogenic arsenic in groundwater poses a serious threat to public health in regions such as the Lake Poopó basin in Oruro, Bolivia. This study developed and evaluated a low-cost experimental filter using metallic iron (Fe^0) and iron oxide (Fe_3O_4) nanoparticles obtained from recycled iron shavings using top-down and bottom-up filtration technologies. The nanoparticles were integrated into a homemade filtration system along with readily available materials such as sand, charcoal, and ground brick. Kinetic and adsorption tests were performed under controlled conditions, achieving arsenic removal rates exceeding 97% with Fe^0 nanoparticles and 91% with Fe_3O_4 . These results best fit the Freundlich isotherm model and second-order kinetics, which describe the arsenate adsorption behavior on both nanoparticles. The filter proved effective for up to 13 consecutive treatment cycles, reducing arsenic concentrations to levels ≤ 0.01 mg/L. This approach represents a sustainable, economical, and technically viable alternative for rural communities affected by this contaminant.

Keywords: Arsenic; Iron nanoparticles; Iron oxide; Groundwater; Low-cost filter; Adsorption

Introduction

Arsenic is an inorganic contaminant naturally present in aquifers of volcanic origin, especially in Andean regions. In Bolivia, its presence in groundwater has been little studied, despite representing a significant health risk. The World Health Organization (WHO) establishes a maximum limit of 10 $\mu\text{g/L}$ for arsenic in drinking water. However, concentrations of up to 112 $\mu\text{g/L}$ have been detected in the community of San Agustín de Puñaca. In groundwater bodies, arsenic is found as hydrogen arsenate and arsenic acid, which, under oxidizing or reducing conditions, can release As^{+5} or As^{+3} ions, respectively. The availability and transport of these compounds in the environment are mainly determined by the pH of the groundwater and by interaction with soil minerals through adsorption and desorption processes. In this context, an experimental filter based on recycled nanomaterials was developed as an accessible and effective solution for arsenic removal. The behavior of Fe^0 and Fe_3O_4 nanoparticles was evaluated using kinetic models and adsorption and equilibrium isotherms for arsenic removal in groundwater samples, allowing the determination of whether the mechanism corresponded to physisorption or chemisorption.

Materials and Methods

Water samples were collected at five sampling points. Analyses included

Affiliation:

¹Faculty of Engineering FICAM, Universidad Mayor, Real y Pontificia de San Francisco Xavier de Chuquisaca, Bolivia

*Corresponding author:

Juan Simón Torres Espada, Faculty of Engineering FICAM, Universidad Mayor, Real y Pontificia de San Francisco Xavier de Chuquisaca, Bolivia.

Citation: Juan Simón Torres Espada, Yrene Romina Lazcano Cruz. Arsenic Removal from Groundwater Using Recycled Iron Nanoparticles: Development and Evaluation of a Low-Cost Filter for Rural Communities. *Journal of Nanotechnology Research*. 7 (2025): 27-33.

Received: December 17, 2025

Accepted: December 11, 2025

Published: December 15, 2025

pH, conductivity, turbidity, and anions. (Bicarbonates, phosphate, nitrates, sulfates), cations (silicon, iron), and total arsenic. To determine the initial arsenic concentration, Atomic Absorption Spectrophotometry (AA500) was used. Samples were microfiltered through a 0.45 μm membrane (Hawach Scientific) using a vacuum pump and then acidified with 2–3 drops of 1% (w/v) HNO_3 (trace metal grade). All samples were stored at low temperature (4°C). Arsenic concentrations were measured using an Atomic Absorption Spectrophotometer to assess the filter's adsorption efficiency.

Metallic iron (Fe^0) and iron oxide (Fe_3O_4) nanoparticles were synthesized from iron shavings using top-down and bottom-up physical and chemical methods. (Torres Espada, 2020) The resulting particles ranged in size from 20–200 nm. The filter consisted of a 5×20.6 cm PVC column with 12 layers of filter materials: Fe^0 and Fe_3O_4 nanoparticles, sand, charcoal, and ground brick. (TorresEscalera, 2024) The downward flow was gravity-fed at 0.16 L/h. Batch tests were performed with different concentrations of nanoparticles (10–100 mg), contact times (10–240 min), pH of the natural water solution and 250 RPM. To determine the percentage of arsenic removal. To study the adsorption kinetics of arsenate on metallic iron and iron oxide particles, jar tests were performed at 250 RPM for predetermined intervals (10, 20, 30, 60, 120 and 240 min) during stirring, using 10 and 100 mg of nanoparticles at a pH of 7.86. The best-fitting isothermal and kinetic models were determined according to the coefficient of determination (R^2 value).

Finally, for the isotherm study, experiments were conducted with an initial arsenate concentration of 112 $\mu\text{g/L}$, using a dosage of 10–100 mg for both nanoparticles at 250 RPM for different times (10, 20, 30, and 60 min). An aliquot was taken from each batch and filtered for arsenic concentration analysis of the filtrate. Several fitting models (Langmuir, Freundlich, and Dubinin) were tested to find the best fit between the experimental data and the theoretical behavior.

Results

Table 1 shows the results of the physical and chemical parameters of the well located in the community of San Agustín de Puñaca, northeast of Lake Poopó, in the department of Oruro. The water quality meets the Bolivian standard NB 512 for drinking water, except for the arsenic content. The arsenic content is 112 $\mu\text{g-As/L}$, significantly higher than the limit established by the Bolivian standard NB 512 of 10 $\mu\text{g-As/L}$. The contents of competitive anions—sulfates, nitrates, chlorides, and phosphates—are relatively low, with the exception of silicates.

Arsenic speciation in groundwater was determined by analyzing the redox potential (Eh) versus pH diagram, which established that under oxidative conditions it has an Eh of 98 mV and a natural pH of 7.86 (Figure 1). Arsenate As^{+5} is the dominant species, having an anionic product of HAsO_4^{2-} , which favors its removal through adsorption processes, since it is negatively charged. Neutral H_3AsO_3 at natural pH

Table 1: Physical-chemical characterization of the San Agustín de Puñaca community.

| Parameters | Units | Analytical Method | Results | Permissible limit NB 512 |
|-------------------------|-------------------------|---------------------------------|---------|--------------------------|
| pH | | SM 4500-H / 1992 Potentiometric | 7.86 | 6.5-9.0 |
| Temperature | $^\circ\text{C}$ | SM 2550/1992 | 18.8 | - |
| Electrical Conductivity | $\mu\text{S}/\text{cm}$ | SM 2510 / 1992 Conductimetric | 970 | 1500 |
| Potential | mV | Potentiometric | 98 | - |
| Oxidation-Reduction | | | | |
| Turbidity | NTU | 2130-B-SM Turbidimeter | 3.19 | 5 |
| Alkalinity | mg/L | ASTM D 1057-02 | 150 | 370 |
| Bicarbonates | mg/L | ASTM D 3875-03 | 94 | 370 |
| Chlorides | mg/L | SM 3030-F / 1992 | 0.45 | 250 |
| Sulfates | mg/L | ASTM D 516-02 | 103.1 | 400 |
| Nitrates | mg/L | DIN 38405 T10 mod. | 7.05 | 45 |
| Phosphates | mg/L | Photometric | 0.2 | - |
| Silicates | mg/L | ASTM D 859-05 | 22.77 | - |
| Iron | mg/L | ASTM D 1068-05A | <0.018 | 0.3 |
| Arsenic | mg/L | SM 3030-F / 1992 EAA | 0.12 | 0.01 |

values (between 6 and 9) is not easily removed. Since arsenic is present as HAsO_4^{2-} , it is not necessary to increase the oxidation-reduction potential, Eh, of the contaminated well by aeration, or by the use of chemical reagents to modify the pH, since if the pH is decreased, arsenite As^{+3} will be present as the dominant species, being more toxic, which explains a lower efficiency in arsenic removal systems.

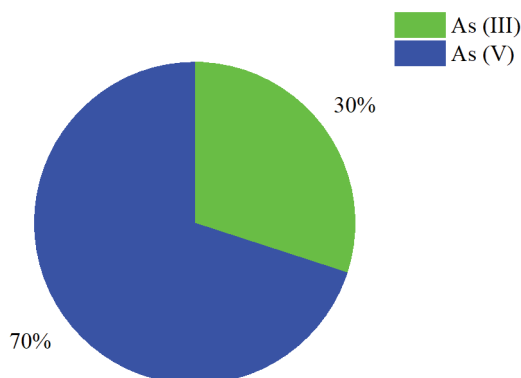


Figure 1: Speciation of arsenic in groundwater.

The filter reduced arsenic to 0.007 mg/L in 13 filtration cycles of 10 L, complying with Bolivian standard NB512 and WHO guidelines. Figure 2 shows the physicochemical characterization of the groundwater sample from the community of San Agustín de Puñaca after filtration, reducing turbidity by 67.08%, Aa by 10%, chlorides by 31.11%, sulfates by 41%, nitrates by 12%, phosphates by 40%, and silicates by 34.46%.

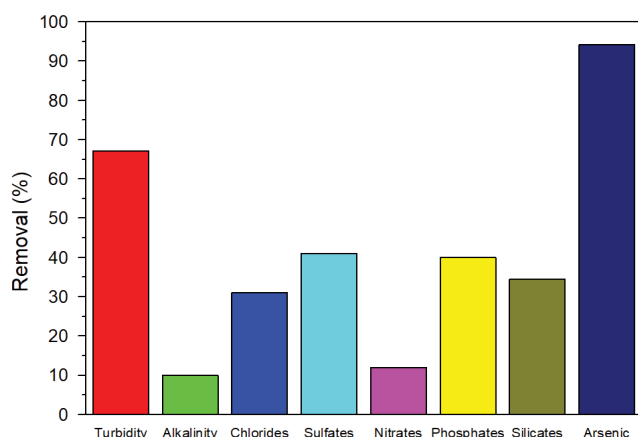


Figure 2: Removal of physicochemical parameters.

The arsenic removal process under these conditions was optimal, achieving a removal rate of 97.5% for (Fe^0) zero valent nanoparticles and 91.7% for Fe_3O_4 iron oxide nanoparticles. The sample was collected directly from its natural environment and contains not only arsenic but also other minerals, organic compounds and other physicochemical properties, including nitrates, silicates, phosphates, sulfates, etc. All these factors, among others, interfere with the adsorption process, making it less efficient.

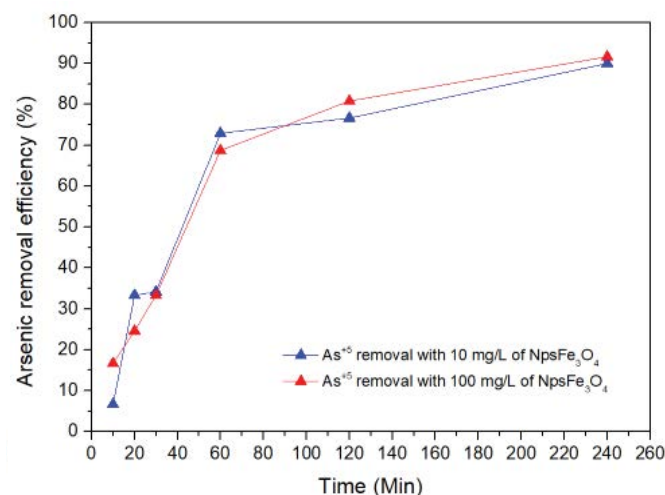
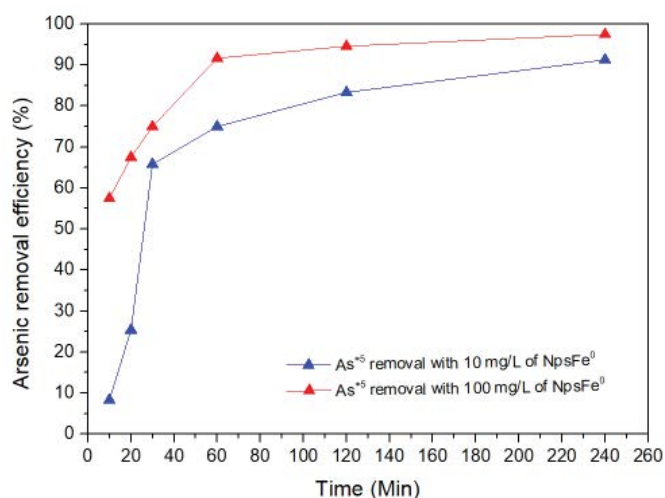


Figure 3: Effect of contact time on arsenic removal efficiency with different doses 10-100 mg a) iron nanoparticles Fe^0 b) iron oxide nanoparticles Fe_3O_4 .

Because the adsorption process was too rapid, exceeding 57.5% efficiency in the first 10 minutes, an equation was developed to describe the adsorption process in such a way that the data could be iterated and the removal efficiency obtained every 2 min, 3 min, 4 min, 5 min, 6 min, etc. It can be seen in Figure 4, that just one minute of contact of the iron nanoparticles with the contaminant, an efficiency of 52% is achieved, thus confirming that the use of metallic iron nanoparticles is effective in the removal of arsenic thanks to their surface area ranging from 60-200 nm, high capacity and high reactivity characteristics of the magnetic material used.

To understand the adsorption mechanism and efficiency of both nanoparticles, the experimental data were analyzed using first-order and second-order kinetic models. The correlation coefficient (R^2) was used to evaluate the best kinetic model (Table 2). Of all the models, the second-order model showed a good correlation coefficient and best fit the experimental data (Figure 5).

Table 2: Kinetic parameters for arsenic removal using metallic iron nanoparticles and iron oxide.

| Kinetic Model | Constant | Worth |
|---|----------------|--------|
| First Order with NpsFe ⁰ | K | -0.017 |
| | R ² | 0.8971 |
| Second Order with NpsFe ⁰ | K | 22,288 |
| | R ² | 0.9607 |
| First Order with NpsFe ₃ O ₄ | K | -0.012 |
| | R ² | 0.9526 |
| Second Order with NpsFe ₃ O ₄ | K | 0.4127 |
| | R ² | 0.9841 |

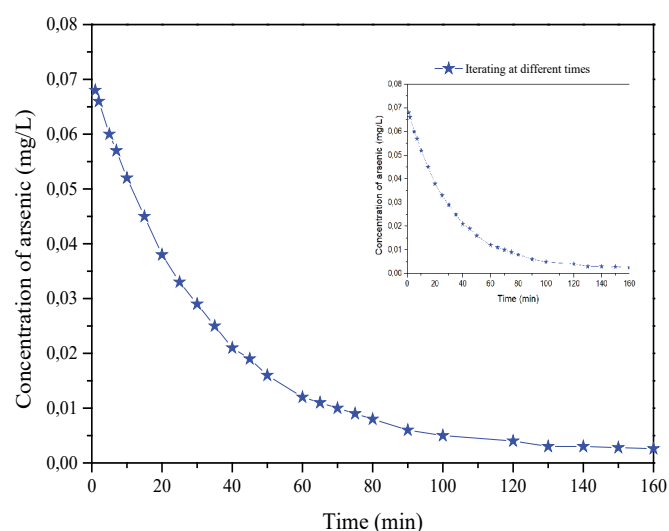


Figure 4: Exponential fit describing the concentration of arsenic in zero valent nanoparticles (Fe⁰).

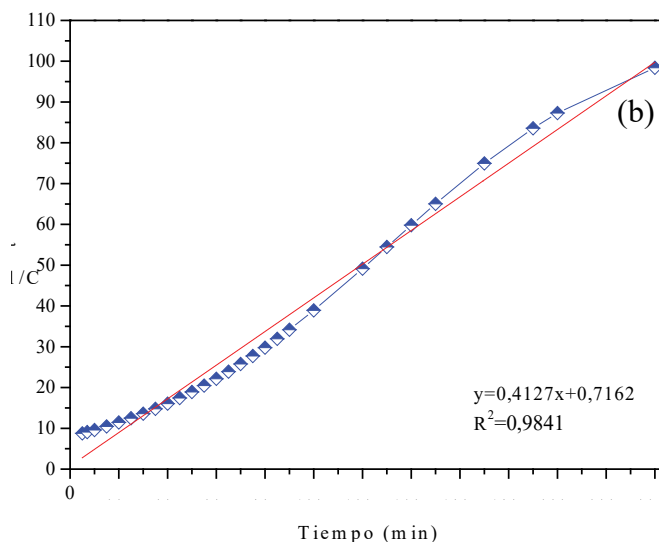
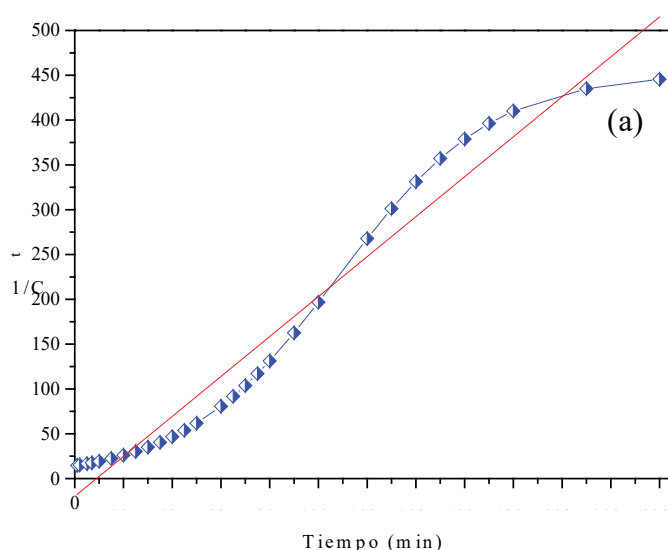


Figure 5: Second-order kinetic model for arsenic removal (a) metallic iron nanoparticles (b) iron oxide nanoparticles.

The half-life with respect to contact time, as shown in (Figure 6), shows that after 180 minutes the nanoparticles no longer adsorb more arsenic, so they begin to saturate and the half-life tends to be constant.

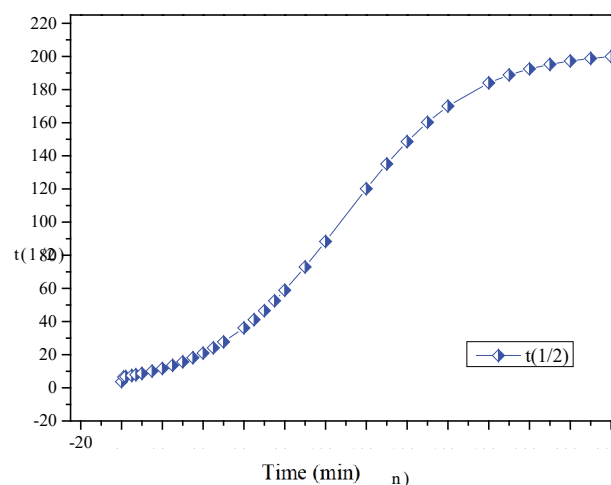


Figure 6: Half-life vs. contact time with NpsFe⁰.

Adsorption isotherm models are fundamental to describing the equilibrium between the adsorbate and the adsorbent. To evaluate the adsorption behavior of the nanoparticles, some well-known isotherms such as the Langmuir, Freundlich, and Dubinin-Radushkevich constants were considered. The fitting results are shown in Figure 7. Table 3 shows the linear regression results according to the Langmuir model. The dimensionless factor R_{L} is less than one; therefore, applying the Langmuir isotherm is unfavorable. The calculated Langmuir constant K_f , which can be interpreted as the enthalpy of adsorption, showed negative

values. This suggested the exothermic nature of the process and indicated that the surface of the metallic iron and iron oxide nanoparticles was energetically favorable for reacting with the ions.

Table 4 shows the results of the Freundlich model; a higher K_f value indicates a greater adsorption capacity of the adsorbent. Furthermore, a K_f value greater than one indicates the spontaneous nature of the process (Mandal et al., 2014). However, for all adsorption isotherms for different quantities of nanoparticles, the regression coefficient R² was more reliable for the Freundlich model, fitting the experimental data better than for the Langmuir model. The value of n is related to the distribution of ions bound to the active sites on the surface of the nano-adsorbent. The negative values of n for the different quantities of nanoparticles indicate that the ions

of the species present are unfavorable, making it impossible to determine whether the process is by physisorption or chemisorption.

Table 5 shows the results obtained after applying the Dubinin model. The regression coefficient was almost the same as those calculated by the Freundlich model.

Thermodynamic parameters, such as Gibbs free energy (ΔG), can help determine the likelihood, spontaneity, or exothermic or endothermic states of a reaction—critical aspects of an adsorption process. The energy required to transfer one mole of metallic iron nanoparticles to iron oxide was greater than 40 kJ/mol for arsenic. These results confirmed that the interactions between the adsorbate and the adsorbent were chemical, i.e., a chemisorption process.

Table 3: Langmuir model results for arsenic adsorption on nanoparticles.

| LANGMUIR MODEL | | | | |
|---|--------------------------------|--------------------------------|---|---|
| | Quantity of NpsFe ⁰ | Quantity of NpsFe ⁰ | Quantity of NpsFe ₃ O ₄ | Quantity of NpsFe ₃ O ₄ |
| PARAMETER | 0.01 g | 0.1 g | 0.01 g | 0.1 g |
| Adsorption capacity of a monolayer | 10,683 | 0.7088 | 10,243 | 0.1789 |
| Q _{or} (mg/g) | | | | |
| Langmuir constant K _f (L/mg) | -33.552 | -26.771 | -30.9536 | -32.8267 |
| Adsorption capacity | 90,000 | 11,000 | 87,500 | 0.825 |
| q _e (mg/g) | | | | |
| Regression coefficient R ² | 0.5863 | 0.7537 | 0.3499 | 0.6984 |
| R _L | -0.3305 | -0.452 | -0.3684 | -0.3402 |

Table 4: Freundlich model results for arsenic adsorption on nanoparticles.

| FREUNDLICH MODEL | | | | |
|---|--------------------------------|--------------------------------|---|---|
| | Quantity of NpsFe ⁰ | Quantity of NpsFe ⁰ | Quantity of NpsFe ₃ O ₄ | Quantity of NpsFe ₃ O ₄ |
| PARAMETER | 0.01 g | 0.1 g | 0.01 g | 0.1 g |
| Freundlich constant K _f (L/mg) | 0.0492 | 0.3372 | 0.044 | 0.0126 |
| Adsorption capacity of a monolayer | 0.2145 | 0.6237 | 0.2576 | 0.1498 |
| Q _e (mg/g) | | | | |
| Adsorption capacity | 90,000 | 11,000 | 87,500 | 0.825 |
| q _e (mg/g) | | | | |
| Regression coefficient R ² | 0.8777 | 0.9189 | 0.7253 | 0.9184 |
| n | -0.6496 | -3.8149 | -0.6199 | -0.7762 |

Table 5: Results of the Dubinin model for the adsorption of arsenic on nanoparticles.

| DUBININ-RADUSHKEVICH MODEL | | | | |
|--|--------------------------------|--------------------------------|---|---|
| | Quantity of NpsFe ⁰ | Quantity of NpsFe ⁰ | Quantity of NpsFe ₃ O ₄ | Quantity of NpsFe ₃ O ₄ |
| PARAMETER | 0.01 g | 0.1 g | 0.01 g | 0.1 g |
| Dubinin constant K _f (L/mg) | 4.47x10 ⁻⁸ | 6.00x10 ⁻⁹ | 4.57x10 ⁻⁸ | 3.18x10 ⁻⁸ |
| Adsorption capacity of a monolayer | 0.3559 | 0.5463 | 0.3745 | 0.06547 |
| Q _e (mg/g) | | | | |
| Adsorption capacity | 90,000 | 11,000 | 87,500 | 0.825 |
| q _e (mg/g) | | | | |
| Regression coefficient R ² | 0.8492 | 0.8877 | 0.6712 | 0.8998 |

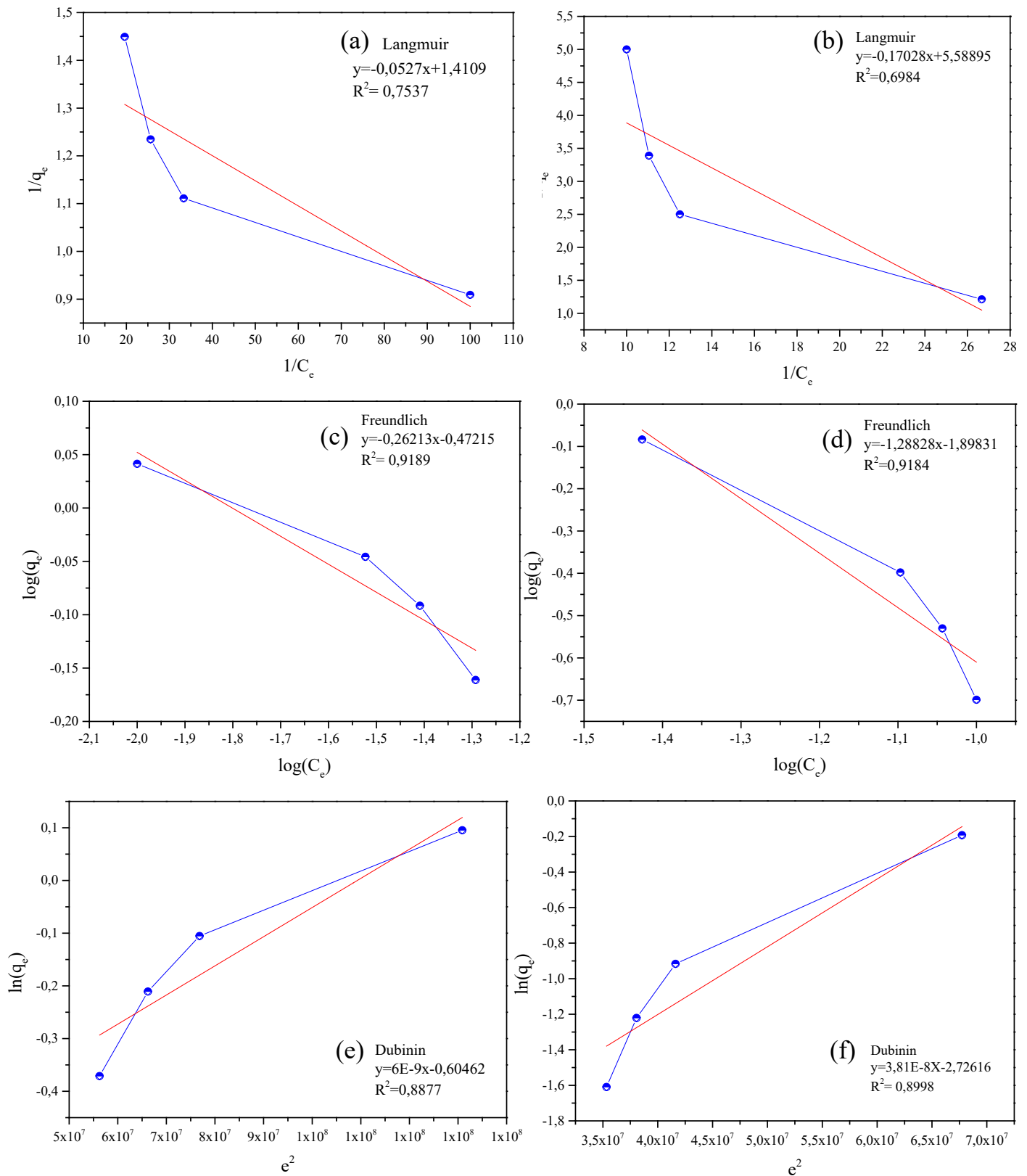


Figure 7: Equilibrium adsorption isotherm for arsenic on metallic iron nanoparticles and iron oxide. (a) Langmuir isotherm with 100 mg of NpsFe⁰. (b) Langmuir isotherm with 100 mg of NpsFe₃O₄. (c) (d) Freundlich isotherm with 100 mg of NpsFe⁰. (e) Freundlich isotherm with 100 mg of NpsFe₃O₄. (f) Dubinin model with 10 mg of NpsFe⁰. (f) Dubinin model with 100 mg of NpsFe₃O₄.

Discussion

The use of recycled nanoparticles represents a technological innovation with a positive environmental and social impact. Despite the small quantities used, the system achieved results comparable to more expensive commercial technologies. Its combination with locally sourced materials facilitates community implementation. The filter also demonstrated the removal of other contaminants (phosphates, silicates, nitrates), increasing its versatility.

Conclusions

- The presence of geogenic arsenic in the community's groundwater was confirmed, in concentrations dangerous to human health.
- The experimental filter developed effectively removed arsenic to levels below that established by the Bolivian standard NB 512 of 10 µg-As/L, making it an accessible solution for rural areas.
- The adsorption fit the Freundlich model and showed second-order kinetics, indicating a chemisorption process and occurring spontaneously.
- The system is replicable, economical and sustainable, with potential for application in other regions with similar problems.

References

1. Carvajal GE. Determination of arsenic in groundwater of the Titicaca sub-basin. 2015.
2. Ravenscroft P, Brammer H, Richards K. Arsenic Pollution: A Global Synthesis. 2009.
3. Muñoz MR. Hydrogeochemistry of naturally occurring arsenic in the Bolivian Altiplano. 2015.
3. Bundschuh J, et al. Distribution of arsenic in Latin America. 2006.
4. (Torres Espada, 2020) Simon, Obtaining iron oxide nanoparticles from chip with bottom-up technology, Revista Ciencia, 18(2021):11-24.
5. T.E.J. Simon, Obtaining iron nanoparticles from chip through top down technology, Int J Green Nanotechnol Mater Sci Eng, 2021.
6. Morgada ME, et al. Arsenic removal with nanoparticulate zerovalent iron. Chemosphere. 2009;143(3):261-8.
7. Ccamercco MH, Falcon NLT. J Environ Health Sci Eng. 2022;20(2):849-860.
7. Mandal, S., Mahapatra, S.S., & Patel, R.K. (2015). Neuro fuzzy approach for arsenic(III) and chromium(VI) removal from water. Journal of Water Process Engineering, 5, 58-75.
8. TorresEscalera. (2024). Iron Nanoparticle Filter for Remediation of Groundwater Contaminated by arsenic. Journal of Drug and Alcohol Research Ashdin Publishing, 7.



This article is an open access article distributed under the terms and conditions of the [Creative Commons Attribution \(CC-BY\) license 4.0](https://creativecommons.org/licenses/by/4.0/)